The MAPKKK Ste11 regulates vegetative growth through a kinase cascade of shared signaling components

Bee Na Lee and Elaine A. Elion*

Department of Biological Chemistry and Molecular Pharmacology, Harvard Medical School, 240 Longwood Avenue, Boston, MA 02115

Communicated by R. L. Erickson, Harvard University, Cambridge, MA, September 1, 1999 (received for review March 22, 1999)

In haploid *Saccharomyces cerevisiae*, the mating and invasive growth (IG) pathways use the same mitogen-activated protein kinase kinase kinase kinase (MAPKKKK, Ste20), MAPKKK (Ste11), MAPKK (Ste7), and transcription factor (Ste12) to promote either G_1 arrest and fusion or foraging in response to distinct stimuli. This exquisite specificity is the result of pathway-specific receptors, G proteins, scaffold protein, and MAPKs. It is currently not thought that the shared signaling components function under the basal conditions of vegetative growth. We tested this hypothesis by searching for mutations that cause lethality when the *STE11* gene is deleted. Strikingly, we found that Ste11, together with Ste20, Ste7, Ste12, and the IG MAPK Kss1, functions in a third pathway that promotes vegetative growth and is essential in an *och1* mutant that does not synthesize mannoproteins. We term this pathway the *STE* vegetative growth (SVG) pathway. The SVG pathway functions, in part, to promote cell wall integrity in parallel with the protein kinase C pathway. During vegetative growth, the SVG pathway is inhibited by the mating MAPK Fus3. By contrast, the SVG pathway is constitutively activated in an *och1* mutant, suggesting that it senses intracellular changes arising from the loss of mannoproteins. We predict that general proliferative functions may also exist for other MAPK cascades thought only to perform specialized functions.

All eukaryotic cells use multiple mitogen-activated protein kinase (MAPK) cascades to respond to external signals to regulate their growth, differentiation, and level of stress (1–3). In *Saccharomyces cerevisiae* haploid cells, four MAPK cascades respond to different external signals to mediate specialized responses (Fig. 1*A*) (1, 4, 5). The mating pathway is activated by peptide pheromones and induces cell-cycle arrest and morphological changes required for mating. The invasive growth (IG) pathway is activated by starvation and induces foraging into agar. The high osmolarity glycerol (HOG) pathway increases intracellular glycerol levels in response to hypertonic stress, whereas the protein kinase C (PKC) pathway maintains cell wall integrity and is activated by hypotonic stress and heat shock.

Surprisingly, subsets of the same kinases are used by the mating, IG, and HOG pathways, even though each pathway has different outputs. The MAPKKKK Ste20 and MAPKKK Ste11 are shared by the mating, IG, and HOG pathways, whereas the MAPKK Ste7 and MAPK Kss1 are shared by the mating and IG pathways (1, 5). Pathway specificity is thought to arise through two major levels of regulation. First, pathway-specific upstream components route the different signals, and pathway-specific MAPKs and transcription factors mediate the different outputs. For example, the pheromone receptors, G protein, Ste5, and Fus3 are specificity factors for the mating pathway, whereas Ras2, Kss1, and the transcription factor Tec1 are specificity factors for the IG pathway (1, 6). Second, the pathways cross-regulate one another to ensure that they are not activated by the wrong signal. For example, Fus3 inhibits misactivation of the IG pathway by mating pheromone (7), whereas Hog1 inhibits misactivation of the mating pathway by hypertonic stress (5, 8).

The analysis of MAPK cascades in yeast and mammalian cells has centered on activities that are induced by a particular external stimulus. Although it is known that the PKC-regulated MAPK cascade has a basal vegetative function that maintains cell wall integrity in the absence of an external stimulus (9), it is currently thought that Ste11 and the downstream kinases in the mating and IG pathways perform specialized functions only in response to their respective stimuli. Here, we show that Ste11 functions under vegetative conditions in a pathway related to the IG pathway that shares functional redundancy with the PKC pathway.

Materials and Methods

Media, Plasmids, and Strains. Yeast extract/peptone/dextrose (YPD) and synthetic complete (SC) media with 2% dextrose were prepared as described (ref. 10, p. 15). Plasmids made for this study are as follows: (*i*) pBL1, a 4.2-kb *Bam*HI–*Xho*I *STE11* fragment from pJD11 (D. Jenness, University of Massachusetts Medical Center, Worcester) in *Bam*HI–*Sal*I sites of pRS313 (P. Hieter, University of British Columbia, Vancouver), (*ii*) pBL2, a 4.2-kb *Bam*HI–*Xho*I *STE11* fragment from pJD11 blunt-ended into the *Sma*I site of pCH1122 (J. Kranz, Brandeis University, Waltham, MA), (*iii*) pBL7, an original *OCH1-URA3-CEN* isolate, (*iv*) pBL12, a 2.6-kb *Sal*I–*OCH1* fragment from pBL7 in pRS315, (*v*) pBL20, a 4.2-kb *Bam*HI–*Xho*I *STE11* fragment from pBL2 in *Bam*HI–*Xho*I sites of pBL15 (*LEU2-ADE3-CEN*). Yeast strains are isogenic to W303a (*ADE3*: EY698, EY699; *ade3*: PY1181, PY1183) or BLY39 [*MAT***a** *ura3–1 leu2–3,112 ade2–1 ade3–1 his3 can1–100 IR*$^+$; made from a cross between PY1181 and L5784 (11)]. All deletion derivatives were made with published deletion plasmids. *och1*Δ was made with pBL-*och1*Δ::*LEU2* (12), which deletes residues 221–951. Details of all strains and plasmids can be obtained from B.N.L. and E.A.E.

Mutant Hunt and Cloning *SLS1/OCH1*. *MAT***a** and *MAT*α W303-derived and *MAT***a** Sigma-derived *ste11*Δ *ade2 ade3 ura3* strains (BLY33, BLY42, BLY39) harboring pBL2 were mutagenized with ethyl methanesulfonate to a 25–45% survival rate, as described (ref. 10, pp. 277–278), and screened for nonsectoring red colonies on YPD plates, as described (13). *sls1–1* (synthetically lethal with *ste11*Δ) was found among 200,000 BLY33 and BLY42 colonies. *sls1–2* was found among 80,000 BLY39 colonies. Four plasmids with inserts overlapping *OCH1* were cloned by restoring sectoring to a *sls1–1 ste11*Δ strain harboring pBL20 (BLY213). *URA3* segregated in opposition to *sls1* in tetrads derived from crosses between a strain with *URA3* integrated into

Abbreviations: MAPK, mitogen-activated protein kinase; IG, invasive growth; HOG, high osmolarity glycerol; PKC, protein kinase C; YPD, yeast extract/peptone/dextrose; DAPI, 4′,6-diamidino-2-phenylindole; SVG, *STE* vegetative growth.

*To whom reprint requests should be addressed. E-mail: elion@bcmp.med.harvard.edu.

The publication costs of this article were defrayed in part by page charge payment. This article must therefore be hereby marked "*advertisement*" in accordance with 18 U.S.C. §1734 solely to indicate this fact.

GENETICS

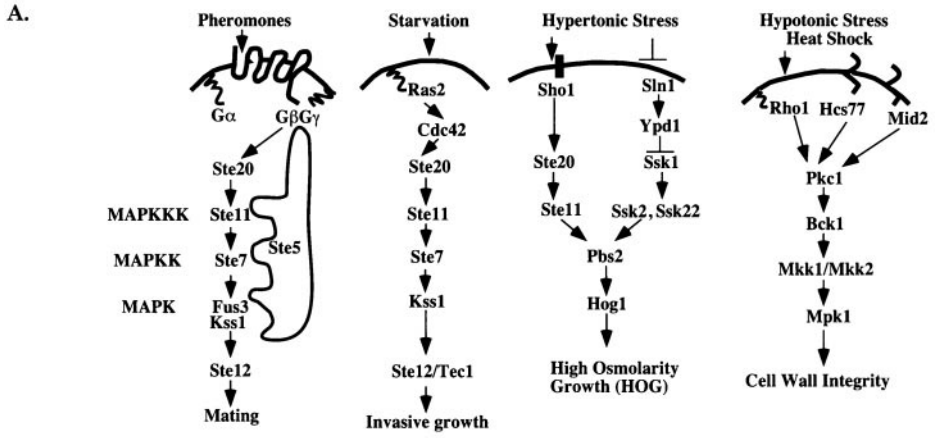

B.

Strain	Phenotype
WT	Healthy (++++)
och1Δ	Slow growth (++)
ste4Δ och1Δ	Slow growth (++)
ste5Δ och1Δ	Slow growth (++)
ras2Δ och1Δ	Slow growth (++)
tec1Δ och1Δ	Slow growth (++)
ste20Δ och1Δ	Lethal (-)
ste11Δ och1Δ	Lethal (-)
ste7Δ och1Δ	Lethal (-)
ste12Δ och1Δ	Very sick (+/-)
fus3Δ och1Δ	Slow growth (++)
kss1Δ och1Δ	Slow growth (++)
fus3Δ kss1Δ och1Δ	Slow growth (++)
fus3-K42R och1Δ	Slow growth (++)
kss1-K42R och1Δ	Very sick (+/-)

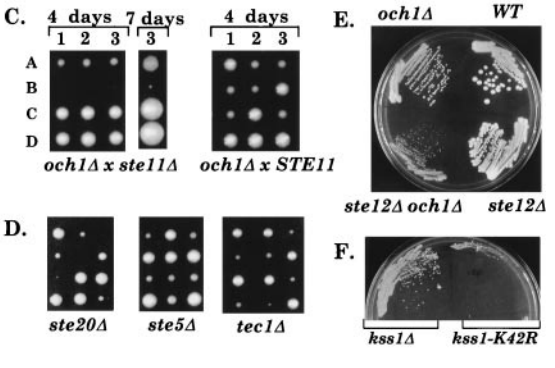

Fig. 1. Summary of genetic interactions with *och1*Δ. (*A*) Four MAPK cascades regulate growth and differentiation in haploid *S. cerevisiae*. (*B*) Summary of genetic interactions. (*C*) *ste11*Δ is synthetically lethal with *och1*Δ. (*Left*) Tetrads from DBL60 (*STE11/ste11*Δ *OCH1/och1*Δ) dissected onto a YPD plate and germinated at 25°C for 4 days. Ascospores 1A–3A are *och1*Δ single mutants, 1B–3B are *ste11*Δ *och1*Δ double mutants. After 7 days, ascospore 3B generates a microcolony of cells that fail to survive. (*Right*) Tetrads from DBL52 (*OCH1/och1*Δ). (*D*) Tetrads from *OCH1/och1*Δ diploids heterozygous for the indicated mutation. (*E*) Streakout of a tetrad from a *ste12Δ/STE12 och1Δ/OCH1* diploid on a YPD plate. (*F*) Streakout (on SC-his) of *kss1Δ sls1Δ* (BLY443) containing vector control (pRS313) or pKSS1K42R-HIS3.

the *OCH1* locus (BLY314) and each *sls1* mutant (BLY216, BLY122), demonstrating linkage between *sls1* and *OCH1*.

Cell Morphology. Cells were grown at 30°C to an OD_{600} of 0.5 in YPD containing 1 M sorbitol. Then they were fixed and stained for DNA with 4′,6-diamidino-2-phenylindole (DAPI), and stained for tubulin with YOL1/34 (Accurate Chemicals), as described (14).

Immunoblots. Invertase was analyzed as described (15) with 5 μl of total protein extract and rabbit anti-invertase antiserum at a 1:1000 dilution (C. Kaiser, Massachusetts Institute of Technology, Cambridge). Kss1, Fus3, and Ste7 were analyzed as described (16). Ste7 was detected with anti-Ste7 rabbit antiserum (B. Cairns, University of Utah, Salt Lake City, UT; 1:10,000 dilution). Phosphorylated Kss1–HA3 and Fus3 were detected with anti-active MAPK Ab (Promega; 1:1500 dilution). Kss1–HA3 was detected with 12CA5 (Harvard University, Boston; 1:10,000 dilution). Tcm1 was detected with anti-Tcm1 mAb (J. Warner, Albert Einstein College of Medicine, Bronx, NY; 1:10,000 dilution). Immunoblots were developed with the enhanced chemiluminescence system (Amersham Pharmacia).

β-Galactosidase Activity. Cells were grown to $<4 \times 10^6$ cells per ml, normalized to equal density, and then grown for 3 hr to $2–4 \times 10^6$ cells per ml (OD_{600} = 0.5–0.6). Extracts were made from 20 ml of cells as described (17).

Double- and Triple-Mutant Constructions. Genes were either deleted in an *och1*Δ/*OCH1* diploid or introduced through crosses. All mutations were verified by Southern blot analysis, except *ste* mutations, which were verified by mating tests. Twelve or more tetrads were analyzed in each cross. All tetrads were dissected onto YPD plates, both in the absence and in the presence of osmotic support (0.3 M KCl, 1 M sorbitol, or 0.1 M sorbitol) and incubated at 25°C. Growth phenotypes were judged by ascospore germination and streaking of cells on YPD plates, with or without osmotic support. 0.1 M sorbitol was used for *bck1*, *pbs2*, and *hog1* mutants to bypass problems of germination and recovery of suppressors for *bck1* mutants without inhibiting the growth of *pbs2* and *hog1* mutants (5).

Results

***STE11* Is Required for Vegetative Growth in *och1* Mutants.** We performed a synthetic lethal screen to identify mutants that require Ste11 for survival. Two mutations were isolated that caused lethality in *ste11* null mutants in both W303a and Sigma (IG+) backgrounds. Both mutations caused slow growth and temperature sensitivity at 37°C. Subsequent analysis showed the mutations were recessive and allelic to *OCH1* (14), so we will refer to them as *och1–1* and *och1–2*. *STE11* was essential for the survival of an *och1*Δ deletion mutant (see *Materials and Methods*). *och1*Δ *ste11*Δ double-mutant progeny derived from an *och1*Δ/*OCH1 ste11*Δ/*STE11* heterozygous diploid were inviable, although *och1*Δ single mutants could grow at permissive temperature (Fig. 1*C*). Approximately 90% of the *och1*Δ *ste11*Δ

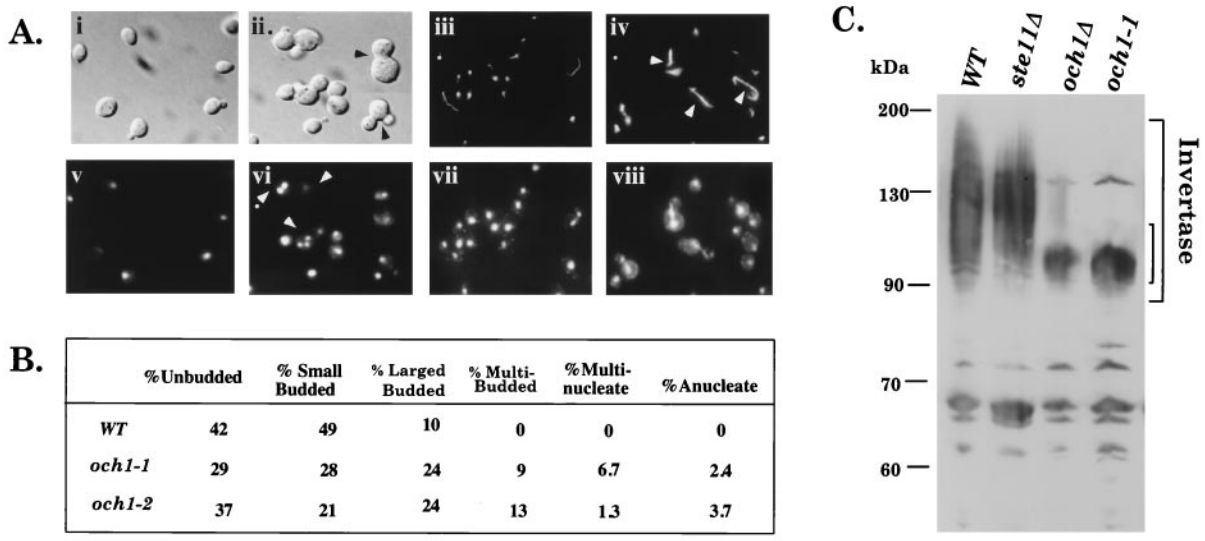

B.

	%Unbudded	% Small Budded	% Larged Budded	% Multi-Budded	%Multi-nucleate	%Anucleate
WT	42	49	10	0	0	0
och1-1	29	28	24	9	6.7	2.4
och1-2	37	21	24	13	1.3	3.7

Fig. 2. *och1*Δ mutants have cell division and glycosylation defects. (*A*) Morphology of *och1* cells. Wild-type (PY1181) panels are *i*, *iii*, *v*, and *vii*. *och1–1* (BLY77) panels are *ii*, *iv*, *vi*, and *viii*. (*i* and *ii*) Nomarski optics. (*v* and *vi*) Parallel DAPI staining. (*iii* and *iv*) Tubulin detected with YOL1/34. (*vii* and *viii*) Parallel DAPI staining. (*B*) Cell-cycle tally of wild-type and *och1* cells. Strains are wild type (PY1181), *och1–1* (BLY77), and *och1–2* (BLY118). Similar results were found for *och1*Δ. (*C*) Immunoblot of invertase from wild type (PY1181), *ste11*Δ (BLY21), *och1*Δ (BLY315), and *och1–1* (BLY77).

double mutants either failed to germinate or ceased dividing after one or two cell divisions, whereas ≈10% germinated and formed a microcolony of cells that could not be propagated, even in the presence of osmotic stabilizers that suppressed the *och1* temperature-sensitive defect. Thus, *STE11* is essential for vegetative growth in an *och1* mutant.

***STE20*, *STE7*, and *STE12* Are Required for Vegetative Growth in an *och1* Mutant.** Remarkably, null mutations in the other signaling components that are shared by the mating and IG pathways also interfered with the growth of the *och1*Δ strain (Fig. 1*B*, representatives shown in *D–E*). *ste20*Δ and *ste7*Δ mutations caused synthetic lethality, whereas the *ste12*Δ mutation caused synthetic sickness. In sharp contrast, null mutations in the mating-specific components *STE4* and *STE5* and the IG-specific components *RAS2* and *TEC1* had no effect on the growth of the *och1*Δ strain. These results suggest that Ste20, Ste11, and Ste7 kinases regulate vegetative growth in a pathway that bifurcates at Ste7, with one branch involving activation of the Ste12 transcription factor. Because mating- and IG-specific components were not required for the survival of the *och1*Δ mutant, Ste20, Ste11, Ste7, and Ste12 must function in a distinct signal-transduction pathway during vegetative growth, which we will refer to as the *STE* (sterile genes) vegetative growth (SVG) pathway.

***och1* Mutants Have Cell-Integrity and Cell-Division Defects.** To determine the function of the SVG pathway, we analyzed the phenotype of *och1*Δ mutants. *OCH1* encodes an α-1,6-mannosyltransferase that initiates outer-chain elongation during N-linked glycosylation in the Golgi (12). Och1 is essential for the synthesis of cell wall mannan, in addition to other mannosylated proteins (12). Phenotypic analysis showed that *och1* mutants had reduced cell wall integrity, consistent with the loss of mannan (data not shown). *och1* mutants were hypersensitive to agents that interfere with cell wall integrity (i.e., calcofluor white, hygromycin B, and SDS), and more *och1* cells appeared as lysed cell ghosts that stained with methylene blue. In addition, growth defects of *och1* mutants were suppressed by osmotic stabilizers (1 M sorbitol and 0.3 M KCl) and overexpression of PKC (*PKC1*).

Additional analysis suggested that Och1 is required for other aspects of vegetative growth. *och1* cells had cell-division defects, as shown by increased percentages of multibudded cells, large-budded cells, multinucleate and anucleate cells, as well as more elaborate microtubules (particularly in cells that failed to properly segregate their nuclei; Fig. 2 *A* and *B*). These defects were not rescued by osmotic stabilizers. *och1* haploids also accumulated less glycogen than did wild-type haploids, and *och1*/*och1* diploids sporulated at reduced efficiency (data not shown). Thus, *och1* mutants had many defects, any of which could overlap with the SVG pathway.

The SVG Pathway Regulates *FKS2*, a Cell Wall Gene. Microscopic examination of the *och1*Δ *ste11*Δ double-mutant progeny that germinated did not provide clues as to the possible function of the SVG pathway because they resembled the *och1*Δ single mutant. In addition, Ste11 was not required for the transcription of either *OCH1* or its homolog, *HOC1* (18), during vegetative growth (data not shown), nor was it required for N-linked outer-chain elongation as assessed by the mobility of secreted invertase on SDS gels (Fig. 2*C*; the sharper and faster mobility of invertase from *och1* mutants is because of the absence of outer-chain mannose).

We tested whether the SVG pathway regulates cell wall integrity through transcriptional activation of genes required for the synthesis of either glucan or chitin, which form the cell wall with mannan (19). This possibility was suggested by the observation that osmotic support rescued the poor growth of an *och1*Δ *ste12*Δ double mutant (data not shown). Of several genes tested, *FKS2* was found to be positively regulated by Ste11 during vegetative growth (Fig. 3*A*). *FKS2* encodes a subunit of (1,3)-β-glucan synthase that functions redundantly with the more abundant Fks1 (1,3)-β-glucan synthase (20). *FKS2* expression was reduced ≈2- to 3-fold in *ste20*Δ, *ste11*Δ, *ste7*Δ, and *ste12*Δ mutants, with no reduction in a *ste5*Δ mutant (Fig. 3*A*). Moreover, *FKS2* expression increased 44-fold in a *STE11–4* strain expressing a constitutively activated form of Ste11 (21), and this increase required *STE12* (Fig. 3*A*). Thus, the SVG pathway operates during vegetative growth in wild-type cells and may play a role in regulating cell wall integrity. The SVG pathway regulates additional targets besides the *FKS2* gene, because a

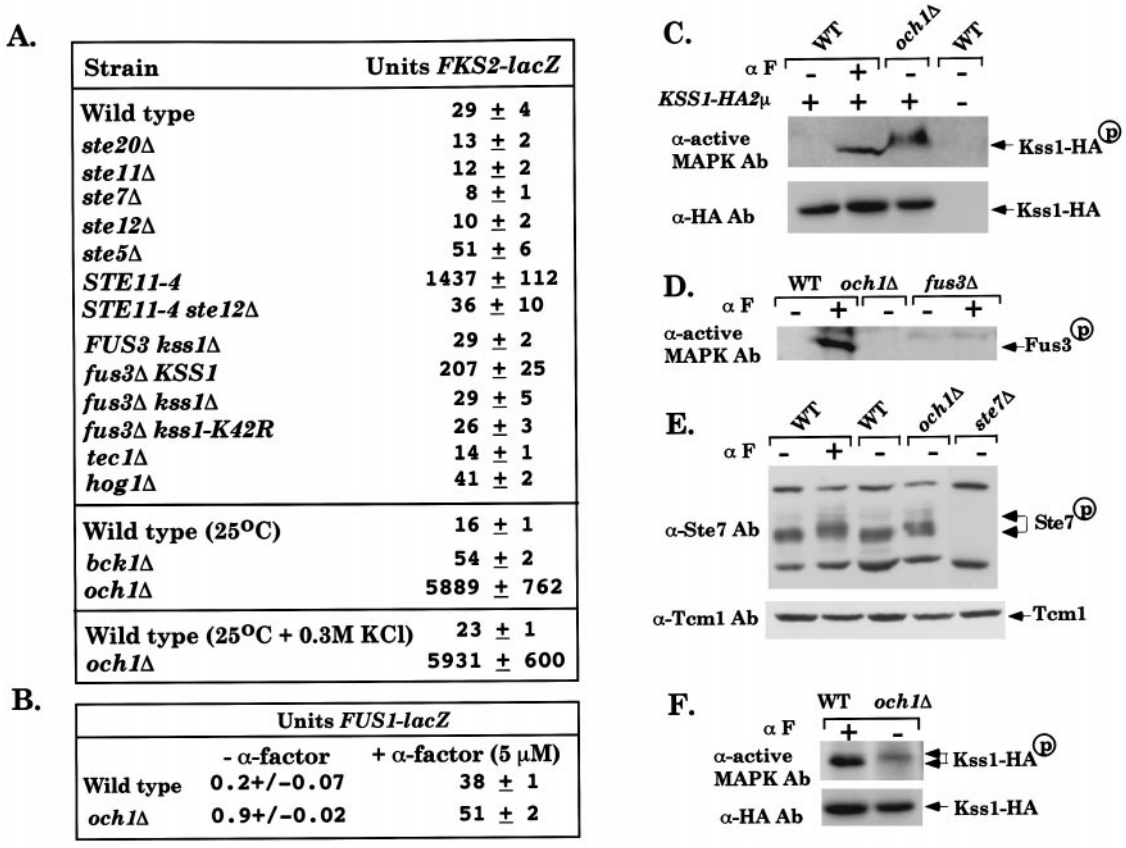

Fig. 3. The SVG pathway regulates *FKS2* and is activated in an *och1* mutant. (*A*) *STE20*, *STE11*, *STE7*, *STE12*, and *TEC1* are required for *FKS2* expression. Strains: PY1181 (WT), BLY409 (*ste20*Δ), BLY21 (*ste11*Δ), FP56 (*ste7*Δ), BLY380 (*ste12*Δ), BLY263 (*ste5*Δ), EY1298 (*STE11–4 far1*Δ), BLY426 (*STE11–4 ste12*Δ *far1*Δ), BLY405 (*kss1*Δ), BLY407 (*fus3*Δ), EY966 (*fus3*Δ *kss1*Δ), BLY535 (*fus3*Δ *kss1*Δ + pKSS1K42R-HIS3), BLY369 (*tec1*Δ), BLY457 (*hog1*Δ), C699-59 (*bck1*Δ), and BLY 341 (*och1*Δ). All strains contained *FKS2-lacZ* on a 2μ plasmid (pDM5) (33) and were grown in SC − uracil at 30°C or at 25°C, with or without 0.3 M KCl where indicated. β-Galactosidase activity (Miller units) was assayed in triplicate, and the average ± SD of three experiments is shown. (*B*) *FUS1-lacZ* expression is not induced in the *och1*Δ mutant. PY1181 (WT) and BLY470 (*och1*Δ) containing *FUS1-lacZ* on a *CEN* plasmid, induced for 120 min with α factor. (*C*) Kss1-HA3 is constitutively phosphorylated in the *och1*Δ mutant. Kss1-HA3 is on a 2μ plasmid (7). α F indicates α factor. The altered mobility of Kss1-HA3-P from the *och1*Δ strain is because of gel conditions (see *F*). (*D*) Fus3 is not phosphorylated in the *och1*Δ mutant. (*E*) Ste7 is hyperphosphorylated in an *och1*Δ mutant. Arrows indicate the portion of Ste7 that is shifted upward in lanes 2 and 4. (*F*) Mobility of phosphorylated Kss1-HA3 in *OCH1* and *och1*Δ strains. Samples in *C*, *D*, and *F* are 50% saturated ammonium sulfate cuts of 2 mg of whole cell extract. Samples in *E* are 50 μg of whole cell extract.

*fks2*Δ mutation did not impair the growth of an *och1*Δ mutant (data not shown).

Kss1 Is the SVG Pathway MAPK. We next tested whether one or both of the MAPKs that regulate mating and IG function in the SVG pathway. MAPK dependency was tested by comparing the effects of *FUS3/KSS1* null mutations with those of catalytically inactive kinases. Growth of the *och1*Δ mutant was not impaired by null mutations in *FUS3/KSS1* or by a catalytically inactive form of Fus3 (encoded by *fus3-K42R*). In contrast, catalytically inactive forms of Kss1 (encoded by *kss1-K42R*, *kss1-T183M*, and *kss1-Y185F*) severely inhibited growth, as found for the *ste12*Δ mutation (Fig. 1 *B* and *F*, and data not shown). Thus, Kss1 functions in at least one branch of the SVG pathway, similar to the IG pathway.

FKS2 expression was elevated 7-fold in a *fus3*Δ mutant, indicating that Fus3 inhibits the SVG pathway during vegetative growth (Fig. 3*A*). By contrast, Kss1 positively regulated *FKS2* expression, as shown by greatly reduced *FKS2* expression in *kss1*Δ *fus3*Δ and *kss1-K42R fus3*Δ strains, compared with the *KSS1fus3*Δ strain. Inactive and unactivatable forms of Kss1 (encoded by *kss1-K42R* and *kss1-Y185F*) did not inhibit *FKS2* expression below basal levels, suggesting that Kss1 regulates *FKS2* through both positive and negative functions, as reported for IG genes (7, 22). We therefore tested whether basal expression of *FKS2* requires the Tec1 transcription factor that dimerizes with Ste12 and is regulated by Kss1 in the IG pathway (7, 22, 23). *FKS2* expression was reduced in a *tec1*Δ mutant to the same degree as in the *ste12*Δ mutant, suggesting that Kss1 regulates the *FKS2* gene through effects on Ste12/Tec1.

The SVG Pathway Functionally Overlaps with the PKC Pathway. We next determined whether the SVG pathway is functionally related to the PKC pathway that is essential for cell wall integrity (9). Null mutations in either *BCK1* (MAPKKK) or *MPK1* (MAPK) of the PKC pathway (Fig. 1*A*) were lethal in an *och1*Δ mutant, and overexpression of *PKC1* suppressed the poor growth of an *och1–1* mutant (data not shown). In addition, simultaneous inactivation of the PKC and SVG pathways caused synthetic growth defects. A *bck1*Δ *ste11*Δ strain grew more slowly than a *bck1*Δ strain (Fig. 4 *A* and *E*), and its poor growth was suppressed by osmotic support (Fig. 4*B*). Moreover, a greater number of the *bck1*Δ *ste11*Δ cells lysed compared with the *bck1*Δ cells (Fig. 4*F*). Thus, SVG and PKC pathways provide additive functions that promote cell wall integrity in parallel with Och1. However, *FKS2* expression was not reduced in a *bck1*Δ mutant, but rather was elevated 3-fold (Fig. 3*A*), arguing that the two pathways do not function identically.

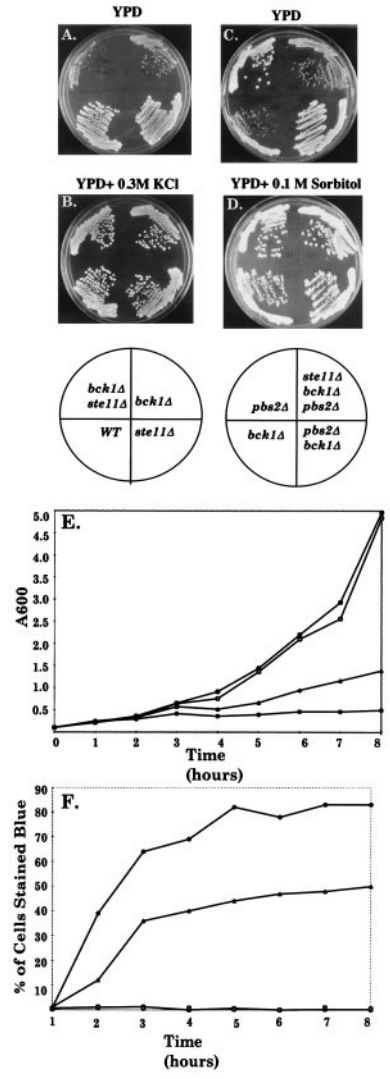

Fig. 4. Genetic interactions between *bck1*, *ste11*, and *pbs2* mutations. (*A*) *ste11*Δ inhibits the growth of a *bck1*Δ strain. (*B*) Rescue of a *ste11*Δ *bck1*Δ double mutant by 0.3 M KCl. (*C*) *pbs2*Δ suppresses a *bck1*Δ strain. (*D*) *bck1*Δ and *bck1*Δ *pbs2*Δ *ste11*Δ strains are rescued by 0.1 M sorbitol. *A–D*, Ascospore progeny derived from DBLY71 (*BCK1/bck1*Δ *STE11/ste11*Δ *PBS2/pbs2*Δ). Plates were incubated at 25°C. (*E*) *ste11*Δ reduces the growth rate of a *bck1*Δ strain. (*F*) *ste11*Δ increases lysis of a *bck1*Δ strain. (*E* and *F*) Strains PY1181 (*STE11*), BLY21 (*ste11*Δ), BLY480 (*bck1*Δ), and BLY478 (*ste11*Δ *bck1*Δ) were grown at 25°C in YPD with 1 M sorbitol medium to logarithmic phase, washed once with YPD medium, resuspended in YPD, and assayed for OD_{600} and methylene blue uptake (0.01% methylene blue in 0.2% sodium citrate and 0.1 M sorbitol). A total of 300 cells were counted for each time point. Strains are wild type (□), *ste11*Δ (■), *bck1*Δ (▲), and *ste11*Δ *bck1*Δ (●).

By contrast, the SVG pathway is functionally distinct from the HOG pathway, which also utilizes Ste20 and Ste11 (Fig. 1*A*). A *pbs2*Δ mutation conferred wild-type growth to the *bck1*Δ mutant instead of a growth defect (Fig. 4*C*; *hog1*Δ gave identical results), and this growth enhancement required Ste11 (compare *pbs2*Δ *bck1*Δ with *pbs2*Δ *bck1*Δ *ste11*Δ). In addition, *FKS2* expression was not reduced in a *hog1*Δ mutant (Fig. 3*A*).

The SVG Pathway Is Constitutively Induced in the *och1* Mutant. We tested whether the SVG pathway is induced in the *och1*Δ mutant that requires it for survival. Remarkably, Kss1 was constitutively phosphorylated in the *och1*Δ mutant, as shown with an Ab that recognizes phosphorylated MAPKs (Fig. 3*C*, note that very low

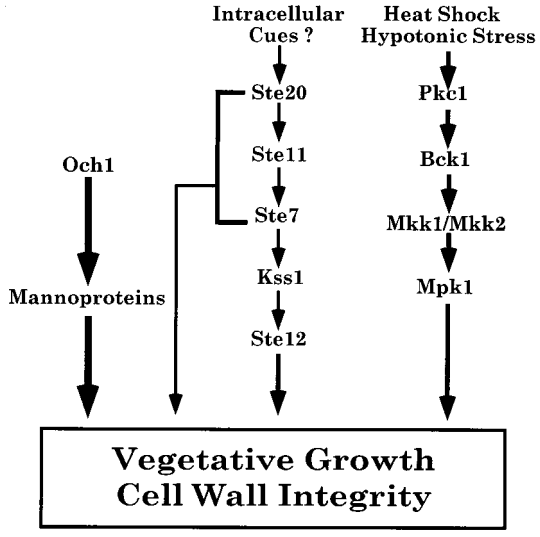

Fig. 5. Model for the control of proliferation by the Ste11 vegetative pathway.

levels of phosphorylated Kss1 could occasionally be detected in the untreated wild-type cells). By contrast, the mating MAPK Fus3 was not phosphorylated in the *och1*Δ mutant (Fig. 3*D*) and was inactive, based on the absence of *FUS1* gene induction (Fig. 3*B*). Kss1 phosphorylation correlated with hyperphosphorylation of Ste7 (Fig. 3*E*), a substrate known to be feedback-phosphorylated by active Fus3 and Kss1 (24), and a 200-fold induction of *FKS2-lacZ* (Fig. 3*A*). Moreover, *FKS2-lacZ* was equivalently induced in osmotic support conditions that suppressed the *och1*Δ growth defect (Fig. 3*A*). Collectively, these results suggest that the SVG pathway is activated as a result of the loss of mannoproteins.

Discussion

Our results lead us to conclude that Ste20, Ste11, Ste7, Kss1, and Ste12 promote normal vegetative growth in a distinct signal-transduction pathway we term SVG for *STE* vegetative growth (Fig. 5). The existence of this pathway is consistent with biochemical analysis showing that both Ste7 and Kss1 have basal kinase activity during vegetative growth (7, 24–26). Basal vegetative functions for these shared kinases provide an additional explanation for the requirement for specificity factors such as Ste5, which may segregate the kinases away from these general constitutive functions.

The SVG pathway is functionally distinct from the mating and IG pathways that also utilize Ste20, Ste11, Ste7, Kss1, and Ste12, based on the absence of a requirement for the pathway-specific genes *RAS2*, *TEC1*, *STE4*, *STE5*, and *FUS3* for the survival of the *och1* mutant. The SVG pathway is also distinct from the HOG pathway, which utilizes Ste20 and Ste11 (5, 27), underscoring its functional specificity. Nevertheless, it seems likely that the SVG pathway is a manifestation of the IG pathway that regulates genes controlled by Ste12/Tec1 heterodimers (23). However, Ste12 must regulate additional genes independently of Tec1 to promote vegetative growth, because Tec1 is not required for vegetative growth in an *och1*Δ mutant.

During vegetative growth, the SVG pathway is inhibited by the same proteins that cross-regulate the mating and IG pathways. Based on *FKS2* expression, Fus3 inhibits the pathway quite strongly, whereas Ste5 modestly inhibits the pathway. Ste5 may inhibit the pathway through sequestration of Ste11 and Ste7 (28). However, possible stimulatory effects from release of Ste11 and Ste7 may be masked by simultaneous release of Fus3, which

inhibits the pathway. Hog1 also modestly inhibits *FKS2* expression as shown for the mating pathway (5, 8). The ability of a *hog1* mutation to suppress the growth defect of the *bck1* null may be partly because of an increase in the activity of the SVG pathway.

Several lines of evidence argue that the SVG pathway functions, in part, to maintain cell wall integrity in parallel with the PKC pathway. First, Ste11 functions in parallel with Och1, which regulates the synthesis of mannan, an important structural component of the cell wall. *och1* mutants have reduced cell wall integrity, and osmotic support suppresses the poor growth of an *och1 ste12* double mutant. Second, Ste11 regulates vegetative growth additively with Bck1, the MAPKKK in the PKC pathway. The poor growth of a *bck1 ste11* double mutant is suppressed by osmotic stabilizers, and *bck1 ste11* double mutants lyse more than *bck1* single mutants (Fig. 4). Third, the SVG pathway positively regulates the expression of *FKS2*, a glucan synthase gene involved in cell wall synthesis (20). The SVG and PKC pathways may regulate vegetative growth through related mechanisms. First, *FKS2* expression is also up-regulated by Bck1 during heat shock through a distinct promoter element (29). Second, a hyperactive form of Ste7 (Ste7P368) can weakly suppress a *bck1* mutant (30). Third, kinases from both pathways interact by two-hybrid analysis with the same morphogenesis proteins, Spa2 and Sph1 (31, 32).

The SVG pathway may have other functions besides cell wall integrity, because Och1 is essential for the N-linked glycosylation of other mannoproteins besides cell wall mannan. For example, *och1* defects in nuclear segregation and microtubule structure may not be indirect consequences of an impaired cell wall (Fig. 2 *A* and *B*). Several observations suggest that the SVG pathway has additional targets besides the control of cell wall integrity (Fig. 5). First, the inviability of an *och1 ste11* double mutant is not remediated by osmotic support, although an *och1 ste12* double mutant is suppressed. Second, although the pathway regulates Tec1, a *tec1* mutation does not impair the growth of an *och1* mutant. Third, two-hybrid interactions between Ste11 and Ste7 and the homologous regulators of polarized morphogenesis Spa2 and Sph1 (31, 32) suggest that Ste11 and Ste7 may regulate morphogenesis.

The constitutive activation of the SVG pathway in the *och1* null (Fig. 3) raises the interesting possibility that the SVG pathway is activated by intracellular signals that arise from structural defects in the cell wall that are the result of the loss of mannoproteins. This possibility is further supported by the observation that *FKS2* expression is also elevated during vegetative growth in both *fks1* and *bck1* mutants that have cell wall defects (29) (Fig. 3). We note that, while the amount of phosphorylated Kss1 appears to be lower in *och1* cells than in wild-type cells treated with α factor, a greater percentage of Kss1 appears to be the slower migrating species of a doublet (Fig. 3*F*). This observation suggests that, on average, a greater percentage of Kss1 has both TEY sites phosphorylated and there may be higher specific activity in the *och1* mutant than in the presence of α factor. Such a scenario would allow the SVG pathway to effect greater change during vegetative growth as a consequence of minor stimulatory events. Further analysis will determine whether the Ste11 vegetative pathway is regulated by physical changes in the cell wall.

To date, the analysis of MAPK cascades in yeast and other organisms has focused on functions and activities that are induced by extracellular signals and routed by specialized regulatory proteins (1, 3). Our analysis suggests that, in *S. cerevisiae*, MAPK cascades also regulate proliferation in addition to specialized functions, through basal levels of activity that may be modulated by intracellular cues to maintain homeostasis. These findings may be applicable to more complex systems and may be important in defining the functions of MAPK cascades in less genetically tractable systems.

We thank J. Broach, K. Cunningham, M. Cyert, B. Errede, G. Fink, D. Levin, Y. Jigami, D. Pellman, H. Saito, P. Silver, and C. Douglas (Merck Research Labs) for generously providing plasmids and strains; J. Horecka for advice on growth of *och1* strains; C. Kaisar for anti-invertase Ab; F. Posas for help with PCR knock outs; and D. Koepp and C. Tai for advice on synthetic lethal screens. We also thank Elion Laboratory members for helpful discussions; and E. Harlow, D. Morisato, D. Pellman, and H. Saito for comments on the manuscript. This work was supported by Leukemia Society of America Fellowship 5583-98 (to B.N.L.) and National Institutes of Health Grant GM4962 (to E.A.E.)

1. Gustin, M. C., Albertyn, J., Alexander, M. R. & Davenport, K. (1998) *Microbiol. Mol. Biol. Rev.* **62,** 1264–1300.
2. Ip, I. T. & Davis, R. J. (1998) *Curr. Opin. Cell Biol.* **10,** 205–219.
3. Widmann, C., Gibson, S., Jarpe, M. B. & Johnson, G. L. (1999) *Physiol. Rev.* **79,** 1–35.
4. Rajavel, M., Philip, B., Buehrer, B. M., Errede, B. & Levin, D. E. (1999) *Mol. Cell. Biol.* **19,** 3969–3976.
5. O'Rourke, S. M. & Herskowitz, I. (1998) *Genes Dev.* **12,** 2874–2886.
6. Elion, E. A. (1998) *Science* **281,** 1625–1626.
7. Madhani, H. D., Styles, C. A. & Fink, G. R. (1997) *Cell* **91,** 673–684.
8. Hall, J. P., Cherkasova, V., Elion, E. A., Gustin, M. C. & Winter, E. (1996) *Mol. Cell. Biol.* **16,** 6715–6723.
9. Levin, D. E. & Bartlett-Heubusch, E. (1992) *J. Cell Biol.* **116,** 1221–1229.
10. Guthrie, C. & Fink, G. R., eds. (1991) *Methods Enzymol.* **194**.
11. Roberts, R. L. & Fink, G. R. (1994) *Genes Dev.* **8,** 2974–2985.
12. Nakayama, K., Nagasu, T., Shimma, Y. & Jigami, Y. (1992) *EMBO J.* **11,** 2511–2519.
13. Bender, A. & Pringle, J. R. (1992) *Mol. Cell. Biol.* **11,** 1295–1300.
14. Elion, E. A., Trueheart, J. & Fink, G. R. (1995) *J. Cell Biol.* **130,** 1283–1296.
15. Kaiser, C. A. & Botstein, D. (1986) *Mol. Cell. Biol.* **6,** 2382–2391.
16. Elion, E. A., Satterberg, B. & Kranz, J. E. (1993) *Mol. Biol. Cell* **4,** 495–510.
17. Farley, F. W., Satterberg, B., Goldsmith, E. J. & Elion, A. E. (1999) *Genetics* **151,** 1425–1444.
18. Neiman, A. M., Mhaiskar, V., Manus, V., Galibert, F. & Dean, N. (1997) *Genetics* **145,** 637–645.
19. Cid, V. J., Duran, A., Rey, D. F., Synder, M. P., Nombela, C. & Sanchez, M. (1995) *Microbiol. Rev.* **59,** 345–386.
20. Mazur, P., Morin, N., Baginsky, W., el-Sherbeini, M., Clemas, J. A., Nielsen, J. B. & Foor, F. (1995) *Mol. Cell. Biol.* **15,** 5671–5681.
21. Stevenson, B. J., Rhodes, N., Errede, B. & Sprague G. F., Jr. (1992) *Genes Dev.* **6,** 1293–1304.
22. Cook, J. G., Bardwell, L. & Thorner, J. (1998) *Nature (London)* **390,** 85–88.
23. Madhani, H. D. & Fink, G. R. (1997) *Science* **275,** 1314–1317.
24. Zhou, Z., Gartner, A., Cade, R., Ammerrer, G. & Errede, B. (1993) *Mol. Cell. Biol.* **13,** 2069–2080.
25. Bardwell, L., Cook, J. G., Voora, D., Baggott, D. M., Martinez, A. R. & Thorner, J. (1998) *Genes Dev.* **12,** 2887–2898.
26. Ma, D., Cook, J. G. & Thorner, J. (1995) *Mol. Biol. Cell* **6,** 889–909.
27. Posas, F. & Saito, H. (1997) *Science* **276,** 1702–1705.
28. Choi, K. Y., Satterberg, B., Lyons, D. M. & Elion, E. A. (1994) *Cell* **78,** 499–512.
29. Zhao, C., Jung, U. S., Garrett-Engele, P., Roe, T., Cyert, M. S. & Levin, D. E. (1998) *Mol. Cell. Biol.* **18,** 1013–1022.
30. Yashar, B., Irie, K., Printen, J. A., Stevenson, B. J., Sprague, G. F., Jr., Matsumoto, K. & Errede, B. (1995) *Mol. Cell. Biol.* **15,** 6545–6553.
31. Roemer, T., Vallier, L., Sheu, Y. J. & Synder, M. (1998) *J. Cell Sci.* **4,** 479–494.
32. Sheu, Y. J., Santos, B., Fortin, N., Costigan, C. & Synder, M. (1998) *Mol. Cell. Biol.* **18,** 4053–4069.
33. Matheos, D. P., Kingsbury, T. J., Ahsan, U. S. & Cunningham, K. W. (1997) *Genes Dev.* **11,** 3445–3458.